ELSEVIER

Journal of Organometallic Chemistry 501 (1995) 107–115

Journal of Organometallic Chemistry

Combined photoelectron–photoabsorption study of (η-cycloheptatrienyl)(η-cyclopentadienyl)tungsten ☆

Jennifer C. Green [a,*], Malcolm L.H. Green [a], Christian N. Field [a], Dennis K.P. Ng [a], Sergey Yu. Ketkov [b,*]

[a] *Inorganic Chemistry Laboratory, University of Oxford, Oxford OX1 3QR, UK*
[b] *Institute of Organometallic Chemistry, Russian Academy of Sciences, Nizhny Novgorod 603600, Russia*

Received 8 April 1995

Abstract

Gas-phase UV photoelectron spectra of the mixed sandwich complexes W(η-C_7H_7)(η-C_5H_5) and W(η-C_7H_7)(η-C_5H_4Me) and photoabsorption spectra of W(η-C_7H_7)(η-C_5H_5) have been measured. The first ionization band of the photoelectron (PE) spectra, assigned to the $^2A_1$ ion state is very sharp, indicating a non-bonding orbital. The second band assigned to the $^2E_2$ ion state shows a splitting of 0.35 eV, the low ionization energy component being 1.5 times the intensity of the higher component. The splitting is primarily due to spin–orbit coupling, but the unequal intensities indicate that the Ham effect is operative with Jahn–Teller distortion of the C_7H_7 ring competing to lift the degeneracy of the $^2E_2$ ion state. The gas-phase electronic absorption spectrum shows comparatively sharp Rydberg bands which disappear in the solution spectrum. All Rydberg excitations originate from the non-bonding metal 5d(a_1, σ^+) orbital. A complete interpretation of the Rydberg structure has been given. In the short-wavelength pattern of the spectrum there are three Rydberg series with quantum defects of 3.26, 3.04 and 2.82 arising from the R*n*p(π), R*n*p(σ^+) and R*n*d(π) transitions respectively. The convergence limit of these series lies at 5.53 eV, being in good agreement with the value for first ionization potential of W(η-C_7H_7)(η-C_5H_5) determined by PE spectroscopy. Below 37 000 cm^{-1}, the spectrum reveals several peaks which were assigned on the basis of their term values to the R6s(σ^+), R6p(π), R6p(σ^+), R6d(π) and R7p(π) transitions. The R6p(π) state shows unusual splitting arising from the spin–orbit coupling induced by an admixture of the valence-shell excited states derived from d–d transitions. The vibronic structures of low-lying Rydberg bands has been analysed.

Keywords: Photoelectron spectroscopy; Tungsten; π-complexes; Sandwich compounds; Photoabsorption; Electronic structure

1. Introduction

The analysis of electronic structures of transition metal sandwich systems with two parallel planar carbocyclic ligands plays an important role in understanding the nature of ligand–metal bonding in many classes of organometallic compounds. Ultraviolet photoelectron (PE) and photoabsorption spectroscopies are the most useful experimental techniques available for studying the order, symmetry and composition of occupied and vacant molecular orbitals (MOs) of such systems. Gas-phase PE spectra have been measured and interpreted previously for a wide number of sandwich complexes [1–14], the majority of studies dealing with derivatives of the first-row and second-row transition metals. The mixed C_7C_5 sandwich compounds have recently been the subject of an extended study using variable-photon-energy PE spectroscopy [14]. This enabled an estimate to be made of the covalent mixing in the e_2 (δ) MO. Another method of estimating the metal character of this MO is by measuring the spin–orbit splitting of the $^2E_2$ ion state formed on ionizing the $(e_2)^4$ configuration. This can normally be resolved for third-row transition metals in a PE experiment [1,3,7–9]. The recent synthesis of (Ch)(Cp)W and (Ch)(Cp′)W, where Cp = (η-C_5H_5), Cp′ = (η-C_5H_4Me) and Ch = (η-C_7H_7), gives us the opportunity to obtain an independent estimate of the metal character of the e_2 interaction.

☆ This paper is dedicated to Professor Herbert Schumann with many thanks.

* Corresponding author.

SSDI 0022-328X(95)05641-6

Valuable information about low-lying vacant MOs of sandwich molecules may be obtained by studying their UV and visible absorption spectra. However, the electronic absorption spectra of transition metal sandwiches in the condensed phase often show only broad structureless bands which cannot be unambiguously assigned, with the exception of d–d transitions in some metallocene systems interpreted on the basis of ligand-field theory [15,16] and ligand-to-metal charge-transfer excitations in a few 16- and 17-electron sandwiches [16–21].

It has been recently found that gas-phase photoabsorption of the compounds considered can reveal comparatively narrow bands which arise from the Rydberg transitions originating at the non-bonding d_{z^2} metal orbital [21–30]. Some sandwich complexes show the Rydberg series converging on an ionization limit [23–30]. Each series is described by the Rydberg formula (Eq. 1).

$$\upsilon_n = I - \frac{R}{(n-\delta)^2} = I - T \qquad (1)$$

where υ_n is the frequency of a series member, I is the energy of ionization from the d_{z^2} orbital, R is the Rydberg constant (equal to 109737 cm^{-1}), n is the principal quantum number of a Rydberg orbital, δ represents the quantum defect, which remains nearly constant within a series, and T is the term value. The T and δ magnitudes represent reliable criteria for assigning Rydberg transitions in sandwich complexes since for each excitation the term value and quantum defect remain almost unchanged within this class of closely related compounds [21–30].

The presence of the Rydberg series makes it possible to determine with high accuracy the ionization potential of a sandwich complex from its photoabsorption spectrum. The study of electronic absorption spectra of such compounds in the gas phase can therefore both give information on the excited states of neutral molecules and supplement the PE data. Previous gas-phase photoabsorption studies of sandwich complexes are concerned mainly with the first- and second-row transition metals (absorption spectra of osmocene and decamethylosmocene only have been studied among the third-row systems [22]).

We describe here a combined gas-phase PE–photoabsorption investigation of a third-row transition metal sandwich. The tungsten compound (Ch)(Cp)W was chosen as an object of our study because its PE and absorption spectra have not been measured up to now while the gas-phase photoabsorption of its chromium analogue (Ch)(Cp)Cr shows very rich Rydberg structure [28].

It has been demonstrated previously [21–30] that comparison of electronic absorption spectra in the gas and solution phases is important for revealing the Rydberg transitions in sandwich molecules. So the study of the (Ch)(Cp)W photoabsorption in solution was carried out in this work in addition to the gas-phase measurements. To analyse the ligand contributions to MOs of the sandwich complex, the spectrum of (Ch)(Cp′)W has also been recorded.

2. Experimental details

(Ch)(Cp)W and (Ch)(Cp′)W were prepared by the literature method [31] and purified by recrystallization from light petroleum (boiling point, 40–60°C) and subsequent vacuum sublimation. Sample purity was checked by NMR and elemental analysis.

The He I and He II PE spectra of (Ch)(Cp)W and (Ch)(Cp′)W were measured using a PES Laboratories 0078 spectrometer by addition of repeated scans on an Atari microprocessor. The samples were held at 110–116 °C and 75–102 °C respectively during data acquisition. The spectra were calibrated using He, Xe and N_2. Band intensities were determined both by integration and by fitting the spectral bands with asymmetric Gaussians. In order to deconvolute the components of bands B and C in the He I spectra, asymmetric gaussians of equal width were taken.

The electronic absorption spectrum of gaseous (Ch)(Cp)W was recorded with a Specord UV–visible (Carl Zeiss, Yena) instrument in an evacuated quartz cell at 100–140 °C. For comparison, the spectrum of the compound dissolved in n-heptane was measured with the same spectrometer in vacuum at room temperature.

3. Results and discussion

3.1. Photoelectron spectroscopy

The ionization energy (IE) region below 12 eV of the He I and He II PE spectra of (Ch)(Cp)W and (Ch)(Cp′)W are shown in Figs. 1 and 2. The fits of asymmetric gaussians to the two components of bands B and C are shown in Fig. 3. Key IE features and band intensities are listed (Table 1). There are four main ionization features, bands A–D, in this region. Bands B and C show two maxima each, labelled B_1, B_2, C_1 and C_2 respectively. On methylation of the cyclopentadienyl ring bands A, B and D show a shift to lower IE of about 0.05 eV whereas band C shows a shift of 0.2 eV. This indicates that band C is mainly cyclopentadienyl in character. Little change is seen in the relative band intensities with photon energy, although band A is somewhat more intense in the He II spectra. Study of the PE cross-section of metal hexacarbonyls shows that W 5d cross-sections fall quite steeply between 20 and 40 eV, at a rate not dissimilar to that of C 2p cross-sec-

tions [32]. Thus no strong differentiation between relative band intensities is expected, and information on the relative metal character of the bands cannot be obtained.

On the assumption of infinite axes of rotation for the carbocyclic rings an MO diagram may be constructed in the $C_{\infty v}$ point group. Fig. 4 presents such a scheme, in which only the interaction of the e symmetry pπ orbitals of the ligands with the metal is considered. In the pseudo-axial ligand field generated by the rings, the metal d orbitals split into three sets; namely d_{z^2} ($1a_1$), d_{xz}, d_{yz} ($3e_1$) and $d_{x^2-y^2}$, d_{xy} ($1e_2$), which are of σ, π and δ symmetries respectively with respect to the metal-ring axes. For (Ch)(Cp)W the orbitals are filled up to the $1a_1$ level.

The ring e MOs become progressively stabilized with increasing ring size, and the energies of these levels with respect to the metal d orbitals are such that an $e_1(\pi)$ interaction is the principal source of (η-C_5H_5)–metal bonding. However the $e_2(\delta)$ MOs provide the more important interaction for the seven-membered ring. The cycloheptatrienyl e_1 orbitals are expected to be the main contributors to the $1e_1$ complex MOs, while the $2e_1$ levels should be predominantly cyclopentadienyl in character.

Of the more metal-based MOs, the $3e_1$ are strongly antibonding while the $1a_1$ MO is largely non-bonding

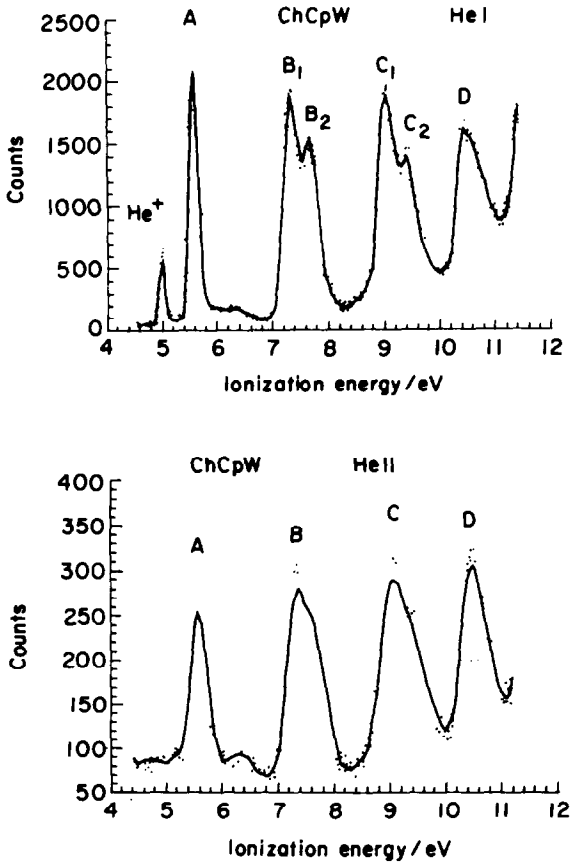

Fig. 1. He I and He II spectra of (Ch)(Cp)W.

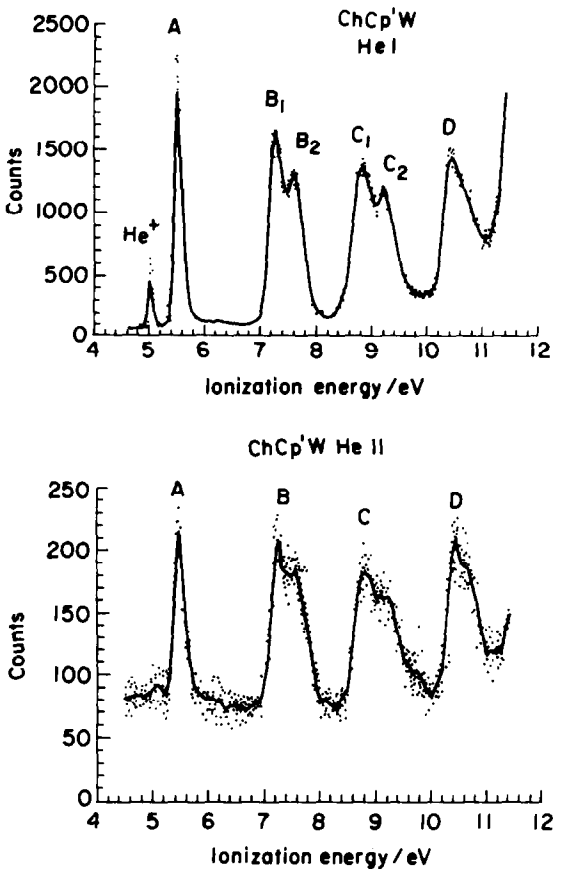

Fig. 2. He I and He II spectra of (Ch)(Cp')W.

(the nodal cone of the d_{z^2} orbital intersects the metal-directed lobes of the C $2p_z$ orbitals of the rings close to their region of maximum electron density [3]. Electron spin resonance evidence strongly supports the metal nd_{z^2} nature of the $1a_1$ MO) [3,13].

The $1e_2$ orbitals are metal → carbon back bonding, and the cycloheptatrienyl e_2 orbital content of these complex MOs is of central importance in determining the nature of the (η-C_7H_7) transition metal bond.

Assignment of bands A–D is straightforward and is given in Table 1. Band B, the $1e_2(\delta)$ ionization shows a definite splitting. A possible origin of this structure is spin–orbit splitting of the $^2E_2$ ion state into $^2E_{5/2}$ and $^2E_{3/2}$ spin–orbit components as a result of a W 5d contribution to the e_2 MO. An analogous splitting is found for example in the PE spectrum of osmocene [6,9]. However, in the latter case the two spin–orbit bands show a greater separation, and are of equal intensity in line with the state degeneracies. In the case of the two W compounds studied here, it is apparent to the eye that the two components are of different intensity. Fitting the spectral band with two equal width asymmetric gaussians gives a relative intensity of 3:2 for $^2E_{5/2}$:$^2E_{3/2}$ in both cases. An alternative mechanism for removing the degeneracy of the $^2E_2$ ion state is Jahn–Teller distortion of the C_7 ring. If this were the

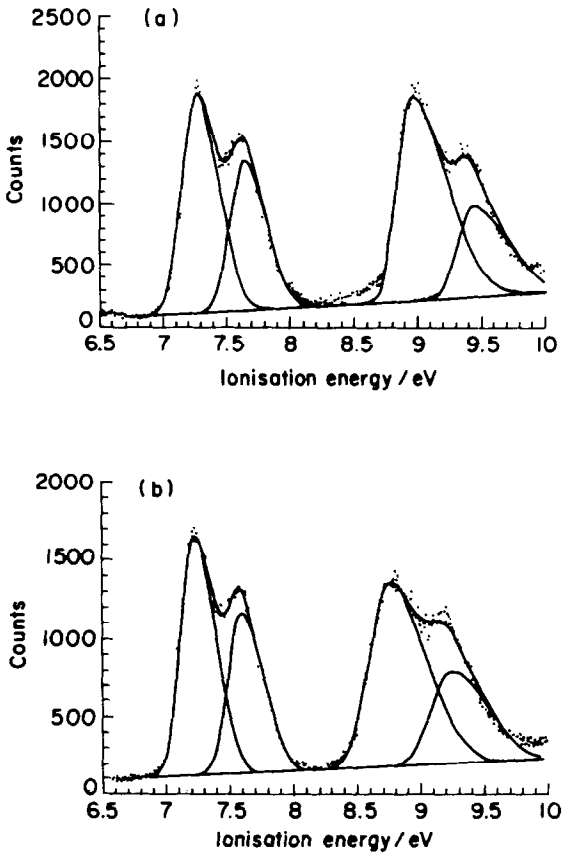

Fig. 3. Fits of asymmetric gaussians to bands B and C of (Ch)(Cp)W and (Ch)(Cp')W.

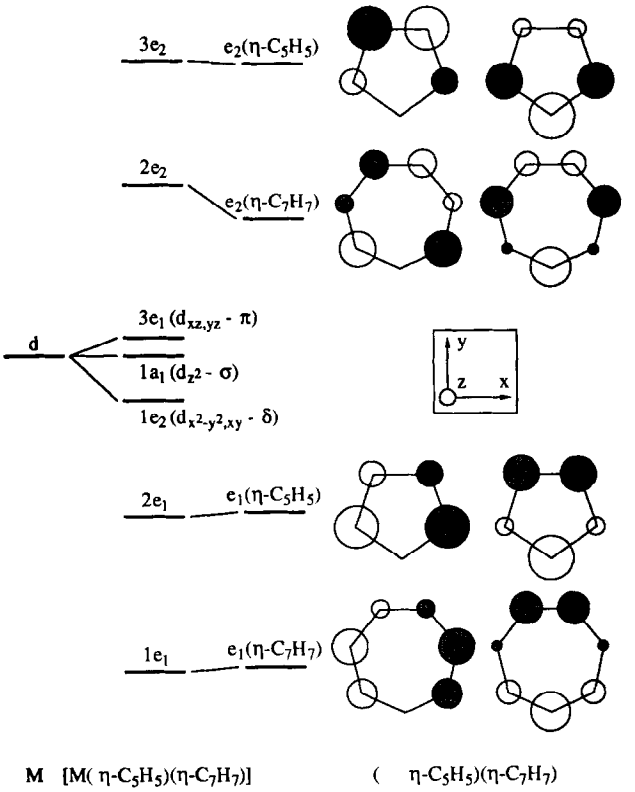

Fig. 4. MO scheme for (Ch)(Cp)W.

only effect operating, a similar band structure would be expected for (Ch)(Cp)Mo but, in this latter case, no high energy shoulder is evident. The most likely explanation of the observed structure is that the Ham effect is operating, whereby spin–orbit splitting and Jahn–Teller distortion are competing to lift the degeneracy [33,34]. In this the qualitative appearance of the energy levels is the same as in the absence of the Jahn–Teller effect, and the splitting of the two states is largely determined by the size of the spin–orbit coupling. The relative intensities differ from the spin–orbit degeneracies as a result of intensity stealing by the vibronic modes. The consequence of the Ham effect for PE bands is best illustrated by the spectra of the methyl halides [35]. The situation found for (Ch)(Cp)W and (Ch)(Cp')W most resembles that of methylbromide where the 2e ionization shows splitting characteristic of Br 4p orbitals but the relative intensities of the $^2E_{3/2}(0–0)$ and $^2E_{1/2}(0–0)$ components are approximately 2 to 1 as opposed to the 1-to-1 ratio expected.

The splitting of the band gives us an estimate of the spin–orbit splitting of the $^2E_2$ ion state which for a pure 5d e_2 orbital is given by 2ζ, where ζ is the atomic spin–orbit splitting of tungsten. A value of 2085 cm^{-1} (0.26 eV) has been estimated for neutral W ζ(5d) [36]. So for a pure d e_2 level we would expect a splitting of 0.52 eV. The experimental value of 0.37–0.38 eV suggests that the e_2 orbital is 71–73% tungsten in character. This may be compared with the values deduced from the previous variable photon energy study of 63% for (Ch)(Cp)Nb and (Ch)(Cp)Mo and 74% for (Ch)(Cp')Ta [14].

Table 1
Ionization energies, band intensities and band assignments for (Ch)(Cp)W and (Ch)(Cp')W

Band	Ionization energy (eV)		He I band intensities		He II band intensities		Assignment
	(Ch)(Cp)W	(Ch)(Cp')W	(Ch)(Cp)W	(Ch)(Cp')W	(Ch)(Cp)W	(Ch)(Cp')W	
A	5.51	5.45	1	1	1	1	$^2A_1$
B_1	7.27	7.23	1.7	1.7	1.9	2.5	$^2E_2$ ($J = \frac{5}{2}$)
B_2	7.65	7.60	1.2	1.2			$^2E_2$ ($J = \frac{3}{2}$)
C_1	8.96	8.75	2.6	2.4	2.4	2.7	$^2E_1$ ($J = \frac{3}{2}$)
C_2	9.43	9.23	1.1	1.2			$^2E_1$ ($J = \frac{1}{2}$)
D	10.40	10.37					$^2E_1$

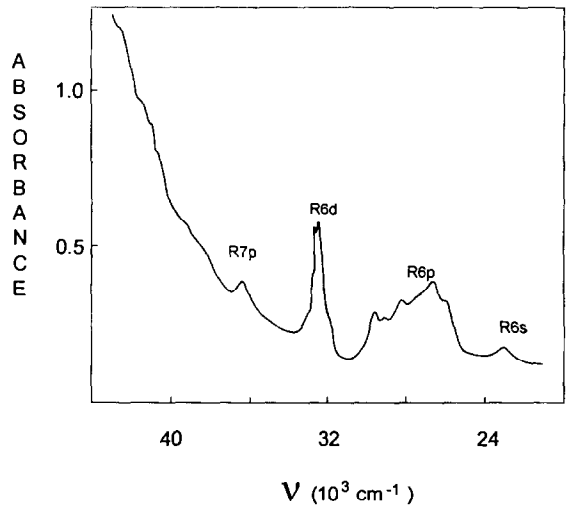

Fig. 5. The electronic absorption spectrum of (Ch)(Cp)W in the gas phase.

The PE spectra of W(η-arene)$_2$ also show two spin–orbit components of unequal intensities for the e_{2g} ionization [3]. Here the separations were found to be 0.43, 0.37 and 0.35 eV for benzene, toluene and mesitylene respectively.

The sensitivity of the IE of band C to substitution on the cyclopentadienyl ring confirms that it has the e_1 orbitals of the C_5 ring as its dominant ligand contribution. Band C also splits the peak separation, being 0.47–0.48 eV. This is too large to be due to any vibrational structure. The relative intensities of the two bands is found in this case to be about 2 : 1 where a pure spin–orbit splitting should give a 1 : 1 ratio. We suggest that the Ham effect is also in operation here. As both W d and p orbitals can mix in the $2e_1$ orbital, we cannot be confident in making a deduction of W 5d character from the size of the splitting. Two facts make us wary of doing this. The cross-section of the analogous band in the spectra of (Ch)(Cp)M where M = Mo, Nb or Ti and that in the spectrum of (Ch)(Cp′)Ta show no marked resonance in the $np \rightarrow nd$ transition, suggesting little 5d character for this orbital. The $^2E_{1u}$ ion state of osmocene shows a similar structure [6,9]. Although the high energy shoulder in this case has been assigned to a C–H stretch [9], a study of deuterated osmocene shows an e_{1u} band with an identical separation [37]. If this structure is also caused by spin–orbit splitting it cannot be assigned to metal d character because of the *ungerade* symmetry of the associated orbital, and must therefore be due to a small admixture of Os *n*p character. Even a small mixing of p character has been shown to produce a significant splitting of a $^2T_2$ ion state in the PE spectrum of OsO_4 [38,39].

An alternative cause of the departure of the intensities of the spin–orbit components from their anticipated intensities could be mixing of states of the same J value. Both the $^2E_2$ and the $^2E_1$ states give $J = \frac{3}{2}$ states as a result of spin–orbit splitting. These are separated by 1.31 eV in $[(Ch)(Cp)W]^+$ and 1.15 eV in $[(Ch)(Cp')W]^+$. Mixing between the two could possibly lead to intensity borrowing by the higher energy state. However, in the case of the bis-arene tungsten compounds the separation of the e_{2g} from the e_{1u}-derived states is greater, making mixing less likely; yet the departure from 1 : 1 intensity in the former is still observed. In addition, the $^2E_{5/2}$ and $^2E_{3/2}$ bands are of equal intensities in the PE spectrum of osmocene and its methylated derivatives, whereas the $^2E_{3/2}$ and $^2E_{1/2}$ components from the e_{1u} ionization are not. Thus a different explanation would have to be operative here. Osmium has a larger 5d spin–orbit coupling constant than tungsten and the cyclopentadienyl ring is a worse δ acceptor than either the C_6 or the C_7 ring; so in the case of the osmium metallocenes the spin–orbit splitting provides the dominant mechanism for lifting the degeneracy. The proposition that the Ham effect is the cause thus explains both the W and the Os results.

Band D is assigned to ionization from the $1e_1$ orbital localized on the C_7 ring.

3.2. Photoabsorption studies

The gas-phase photoabsorption spectrum of (Ch)(Cp)W (Fig. 5) consists of comparatively narrow peaks lying below 37 000 cm^{-1} and weak sharp shoulders superimposed on a strong and very broad absorption band at higher energies. Both peaks and shoulders disappear on going to the solution phase. The solution spectrum (Fig. 6) shows only broad absorption bands E at 42 700, 33 500, 30 500, 27 200 and 24 700 cm^{-1} respectively, bands B–E being too weak to be observed in our gas-phase experiment. In the spectra of polyatomic molecules, the disappearance of sharp absorption features on going from the gas to condensed phase is

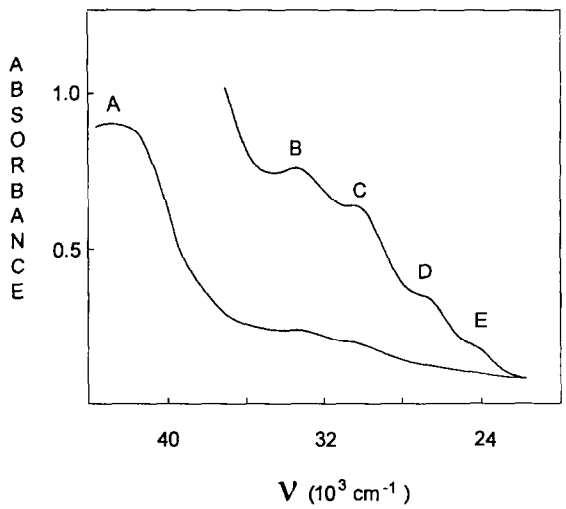

Fig. 6. The electronic absorption spectrum of (Ch)(Cp)W in *n*-heptane solution.

usually indicative of their Rydberg nature [40]. By analogy with the sandwich complexes investigated previously [21–30], it is reasonable to assign the narrow bands in the (Ch)(Cp)W gas-phase absorption spectrum to the Rydberg excitations originating at the non-bonding 5d(σ^+) orbital. The notation of $C_{\infty v}$ point group is used here for designation of the (Ch)(Cp)W MOs and electronic states.

The long-wavelength peaks can be interpreted on the basis of their term values, knowledge of the ionization threshold being necessary to calculate the T magnitudes. With the sandwich complexes revealing clearly defined Rydberg series, the I values were readily determined using Eq. (1) and frequencies of high-lying Rydberg bands [23–30]. Unfortunately, in the gas-phase photoabsorption of (Ch)(Cp)W, the higher Rydberg excitations are observed as very weak shoulders on the background of the strong valence-shell band which transfers into peak A on going to the solution (Fig. 6). This makes it difficult to reveal separate Rydberg series when analysing the photoabsorption of (Ch)(Cp)W alone. It appears to be possible, however, to find Rydberg series in the spectrum of the tungsten compound on the basis of comparison with the spectrum of its chromium analogue (Ch)(Cp)Cr. The gas-phase photoabsorption of (Ch)(Cp)Cr shows three sharp Rydberg series [28]. Weak shoulders of (Ch)(Cp)W seem to match well the members of these series if the spectrum of the tungsten complex is shifted by 560 cm^{-1} to red from that of (Ch)(Cp)Cr (Fig. 7).

In the absorption spectrum of the chromium compound, three series converge on an ionization limit of 45 190 cm^{-1} [28]. We deduce therefore that for (Ch)(Cp)W the ionization threshold lies at 44 630 cm^{-1}

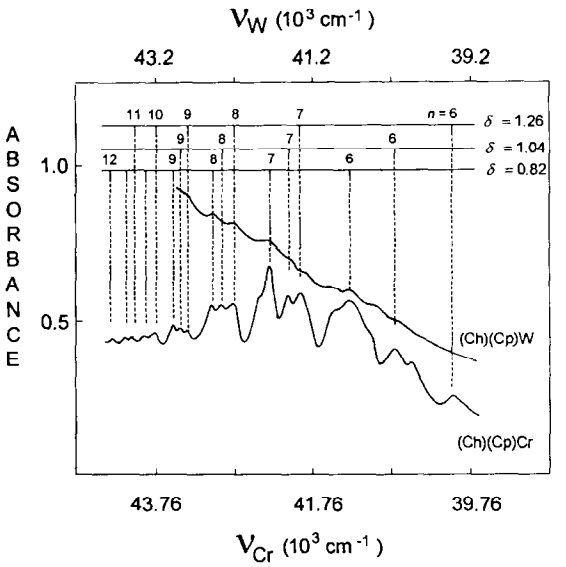

Fig. 7. The short-wavelength pattern of the gas-phase UV absorption spectra of (Ch)(Cp)W (top) and (Ch)(Cp)Cr (bottom). The Rydberg series are shown for the chromium complex.

Table 2
Calculated and observed frequencies of the members of three Rydberg series in the short-wavelength pattern of the (Ch)(Cp)W gas-phase absorption spectrum (Fig. 7)

n	Series 1 ($\delta = 3.26$)		Series 2 ($\delta = 3.04$)		Series 3 ($\delta = 2.82$)	
	ν_{calc} (cm^{-1})	ν_{obs} (cm^{-1})	ν_{calc} (cm^{-1})	ν_{obs} (cm^{-1})	ν_{calc} (cm^{-1})	ν_{obs} (cm^{-1})
8	39750		40170	40130	40540	40700
9	41300	41250	41540	41530	41760	41750
10	42210	42200	42360		42500	42470
11	42800	42800	42900		42990	

or 5.53 eV. The frequencies of the short-wavelength shoulders observed in the (Ch)(Cp)W gas-phase spectrum and those calculated using Eq. (1) with $I = 44\,630$ cm^{-1} are compared in Table 2. It is seen that the experimental ν values coincide with the theoretical values for all bands excepting one member of series 3 ($n = 8$, $\delta = 2.82$) which position is slightly shifted to blue. The corresponding peak in the (Ch)(Cp)Cr spectrum (Fig. 7) is also shifted from the calculated frequency. This peak is broadened owing to admixture of an intravalency transition. So the deviation from the theoretical value is probably a result of interaction between the Rydberg state and a lower-lying valence-shell level. The convergence limit of the three (Ch)(Cp)W Rydberg series is very close to the first ionization potential found in the PE study. This demonstrates the good accordance between our photoabsorption and PE results as well as supporting the assignment of sharp absorption bands to the Rydberg transitions from the 5d(σ^+) orbital. An attempt at a more detailed interpretation of the Rydberg series can be made on the basis of their quantum defects (Table 2).

The principal quantum number of the occupied metal orbital participating in a Rydberg excitation increases by 2 when Cr is replaced by W in a sandwich complex. So the n values in Eq. (1) increase by 2 as well. The quantum defect undergoes the same change as predicted by theory [39]. Consequently, the effective quantum number and term value of a Rydberg transition remain constant on going from the chromium to the tungsten sandwich. The series characterized by $\delta = 3.26$ in (Ch)(Cp)W and $\delta = 1.26$ in (Ch)(Cp)Cr corresponds to that with $\delta = 1.35$ in a bis-benzene analogue $(Bz)_2Cr$ ($Bz = \eta$-C_6H_6) [26] which arises from the excitations terminating at Rydberg $np(\pi)$ orbitals. The quantum defect of 3.04 (series 2) is appropriate for assigning the series to the 5d(σ^+) → Rnp(σ^+) or 5d(σ^+) → Rnd transitions. For the Rnp(σ^+) series in $(Bz)_2Cr$ the quantum defect was found to be 1.12 [26]. Series 3 in (Ch)(Cp)W ($\delta = 2.82$ ppm) can be considered as being due to the Rnd or Rns excitations (in the latter case, $n + 1$ and $\delta + 1$ should be used instead of n and δ in Table 2).

In the short-wavelength pattern of the (Ch)(Cp)W

Table 3
Frequencies, term values, principal quantum numbers, quantum defects and assignments of long-wavelength Rydberg bands in the spectrum of vaporous (Ch)(Cp)W (Fig. 5)

ν (cm^{-1})	T (cm^{-1})	n	δ	Rydberg state [a]	Vibronic assignment [b]
22900	21730	6	3.75	R6s(σ^+)	0_0^0
25800 [c]	18830	6	3.59	R6s(σ^+)	$1_0^1+2_0^1$
26360	18270	6	3.55	R6p(π)(2)[d]	0_0^0
27930	16700	6	3.44	R6p(π)(5)[d]	0_0^0
28720 [c]	15910	6	3.37	R6p(π)(5)	$3_0^1+4_0^1$
29170	15460	6	3.34	R6p(σ^+)	0_0^0
31380 [c]	13250	6	3.22	R6d(π)	5_2^0
31670 [c]	12960	6	3.09	R6d(π)	5_1^0
31920	12710	6	3.06	R6d(π)	0_0^0
32150	12480	6	3.03	R6d(π)	5_0^1
32380 [c]	12250	6	3.01	R6d(π)	5_0^2
32640 [c]	11990	6	2.97	R6d(π)	5_0^3
35930	8700	7	3.45	R7p(π)	0_0^0

[a] Rydberg states are defined here via corresponding Rydberg MOs.
[b] See text for designation of vibrational modes.
[c] Shoulder.
[d] Spin–orbit components of the $5d(\sigma^+)^1R6p(\pi)^1$ configuration (see text).

gas-phase photoabsorption (Fig. 7), there are also two shoulders at 40430 cm^{-1} ($n-\delta=5.11$) and 40950 cm^{-1} ($n-\delta=5.46$) which do not belong to any of the three Rydberg sequences mentioned above. The quantum defects are appropriate for interpreting these bands as R8d or R9s excitations. Higher-lying Rydberg components corresponding to these transitions are non-observable on the background of more intense members of three main Rydberg series.

Thus there are five types of Rydberg excitation shown by the (Ch)(Cp)W gas-phase absorption spectrum above 37000 cm^{-1}. This is quite possible since the electronic transitions from MO $5d(\sigma^+)$ to the R$ns(\sigma^+)$, R$np(\pi)$, R$np(\sigma^+)$, R$nd(\pi)$ and R$nd(\sigma^+)$ levels are allowed by selection rules under the $C_{\infty v}$ symmetry. Only the R$np(\pi)$ series can be identified unambiguously on the basis of its quantum defect. For other short-wavelength excitations, the δ values are too close to each other to make a concrete assignment. To interpret them, it is necessary to know the parameters of lower-lying series members.

The frequencies of long-wavelength Rydberg peaks of (Ch)(Cp)W are given in Table 3 together with the term values, principal quantum numbers and quantum defects which were calculated using Eq. (1) with $I=$ 44630 cm^{-1}. Taking into consideration the T magnitudes of lower-lying Rydberg excitations in the sandwich molecules investigated previously [21–30], these peaks can be grouped into four blocks as shown in Fig. 5. The R6s, R6p and R7p bands (Fig. 5) are broadened appreciably in comparison with corresponding peaks in the (Ch)(Cp)Cr spectrum [28]. Such broadening might be caused by strengthening of bonding–antibonding properties of the uppermost occupied $d(\sigma^+)$ MO on going from (Ch)(Cp)Cr to (Ch)(Cp)W or by interaction of Rydberg states with valence-shell levels. The former reason, however, is unlikely since sharpness the R6d components (Fig. 1) is indicative of strongly non-bonding character of the $5d(\sigma^+)$ orbital in the tungsten sandwich. The term value of the $5d(\sigma^+)\rightarrow R6s(\sigma^+)$ transition (Table 3) is somewhat larger than that of the lowest Rydberg excitation in (Ch)(Cp)Cr (21390 cm^{-1} [28]). Both the shift in the R6s peak and its broadening is a result of mixing between the R6s state and the higher-lying valence-shell level contributing to band D or E in the solution spectrum (Fig. 6).

It is not a simple problem to interpret the absorption features of the R6p block (Fig. 5). This block consists of three peaks with clearly defined maxima at 26360, 27930 and 29170 cm^{-1} and two shoulders at 25800 and 28720 cm^{-1}. The term value of its highest component (Table 3) is very close to that of the $3d(\sigma^+)\rightarrow R4p(\sigma^+)$ excitation in $(Cp)_2Fe$ (15860 cm^{-1} [21,22]), $(Bz)_2V$ (15650 cm^{-1} [21,26], (Cp)(Ch)Cr (15490 cm^{-1} [28]) and (Cp)(Bz)Mn (15920 cm^{-1} [29,30]). This peak must therefore be assigned to the $5d(\sigma^+)\rightarrow R6p(\sigma^+)$ transition. Then the two other maxima arise from the excitations terminating at MO R6p(π). Instead of one R4p(π) transition with $T=17580$ cm^{-1} in (Ch)(Cp)Cr [28], the spectrum of (Ch)(Cp)W shows two peaks with $T=18270$ cm^{-1} and $T=16700$ cm^{-1} (Table 3). Such a splitting is most probably a result of the spin–orbit coupling caused by the presence of the heavy tungsten atom.

Indeed, the $5d(\sigma^+)^1R6p(\pi)^1$ configuration gives the $^3\Pi$ and $^1\Pi$ states which produce under strong spin–orbit coupling five levels: $\delta(1)$, $\Pi(2)$, $\Sigma^+(3)$, $\Sigma^-(4)$ and $\Pi(5)$ (the $C_{\infty v}^*$ double point group), the states 1–4 coming from $^3\Pi$ and state 5 from $^1\Pi$ [41]. Formally, a similar situation takes place with the $np(e)\rightarrow R(n+1)s(a_1)$ transition in methyl halides (the C_{3v} symmetry) [41–45]. The energy increases from state 1 to state 5, levels 3 and 4 being nearly degenerate. Only transitions to the Π states (i.e. states 2 and 5) are both symmetry and momentum allowed. Accordingly, two intense absorption bands are expected to arise from the $5d(\sigma^+)\rightarrow R6p(\pi)$ excitation as a result of the spin–orbit coupling. So the maxima at 26360 and 27930 cm^{-1} should be assigned as the promotions to states 2 and 5 respectively. Note, however, that in closed-shell polyatomic molecules degenerate orbitals of ionic core are usually responsible for the spin–orbit splitting [40,46].

It is surprising that the $5d(\sigma^+)^1R6p(\pi)^1$ configuration derived from a non-degenerate state of the (Ch)(Cp)W ionic core splits because of the spin–orbit coupling. In fact, the spectrum of isoelectronic osmocene shows no splitting of the R6p(π) state [22]. A possible explanation is that spin–orbit splitting of the $5d(\sigma^+)\rightarrow R6p(\pi)$ transition in (Ch)(Cp)W is induced by an admixture of valence-shell excitations involving

one or two tungsten-localized degenerate MOs. The $5d(\sigma^+) \rightarrow 5d(\pi)$ and $5d(\delta) \rightarrow 5d(\pi)$ promotions responsible for bands D and E in the solution spectrum (Fig. 6) possess appropriate symmetries and energies of the upper states to be the most probable candidates for mixing with the Rydberg transition considered. The interaction between the $5d(\sigma^+)^1R6p(\pi)^1$ and $5d(\sigma^+)\,^15d(\pi)^1$ configurations can be described as mixing of Rydberg MO $R6p(\pi)$ with its valence-shell conjugate $5d(\pi)$ while the admixture of the $5d(\delta)^1\ 5d(\pi)^1$ state is possible only via configuration interaction [46].

The energy separation of states 2 and 5 and the relative intensities of corresponding transition are predicted to be

$$E(5) - E(2) = 2\left(\zeta^2 + k^2\right)^{1/2}$$

and

$$\frac{f(5)}{f(2)} = \left\{\frac{k}{\zeta} + \left[1 + (k/\zeta)^2\right]^{1/2}\right\}^2$$

respectively, where ζ is the spin–orbit integral and k is the exchange integral [41]. Close intensities of maxima at 26360 and 27930 cm^{-1} indicate that $\zeta \gg k$. Then the spin–orbit coupling constant can be estimated as $\zeta \cong (E(5) - E(2))/2 \cong 0.01$ eV. This value is appreciably lower than that found above from PE ionization of MO $5d(\delta)$. The decrease in the magnitude is due to a much more limited percentage of metal atomic character for the Rydberg $R6p(\pi)$ orbital than for that for the valence-shell $5d(\delta)$ MO.

The intensity of the lowest energy shoulder in the R6p block (Fig. 5) is too high to assign this feature as either the $5d(\sigma^+) \rightarrow R6p(\pi)$ forbidden spin–orbit component corresponding to state 1 or as a hot band arising from the promotion to state 2 or 5. It seems to be more reasonable to interpret the shoulder at 25800 cm^{-1} as a vibronic component of the $5d(\sigma^+) \rightarrow R6s(\sigma^+)$ transition. The vibronic levels of the $R6s(\sigma^+)$ state corresponding to singly excited π or σ^+ vibrations are dipole allowed in the $C_{\infty v}$ group. However, only the π component can "steal" intensity from the strong $5d(\sigma^+) \rightarrow R6p(\pi)$ transition, making the vibronic band at 25800 cm^{-1} more intense than the 0_0^0 peak at 22900 cm^{-1} (Fig. 1), which is unusual for an allowed Rydberg excitation. The shoulder at 25800 cm^{-1} lies 2900 cm^{-1} higher than the 0_0^0 $5d(\sigma^+) \rightarrow R6s(\sigma^+)$ band. This spacing correlates very well with the 2917 cm^{-1} (Ch)(Cp)W IR frequency assigned to the C–H e_1 stretching modes ν_1 and ν_2 of cycloheptatrienyl and cyclopentadienyl ligands [47]. (The normal coordinate analysis of the (Ch)(Cp)M systems has not been carried out and there is no generally used notation of vibrational modes in such complexes. So, to make the vibronic assignments more obvious, we define here only those vibrations which are observed in the structure of Rydberg bands.) The ν_1 and ν_2 modes can be described as π vibrations in the $C_{\infty v}$ point group. It is therefore quite reasonable to assign the shoulder at 25800 cm^{-1} to the 1_0^1 and 2_0^1 components of the $5d(\sigma^+) \rightarrow R6s(\sigma^+)$ excitation which "steal" their intensities from the $5d(\sigma^+) \rightarrow R6p(\pi)$ transition.

The shoulder at 28720 cm^{-1} in the R6p block is separated by 790 cm^{-1} from the maximum at 27930 cm^{-1}. A similar feature was observed in the structure of the $R4p(\pi)$ band in the spectra of $(Bz)_2Cr$, (Ch)(Cp)Cr and (Bz)(Cp)Mn [26,28–30]. The 790 cm^{-1} separation corresponds to excitation of the Ch and Cp totally symmetric C–H umbrella vibrations ν_3 and ν_4 in the $R6p(\pi)(5)$ state of (Ch)(Cp)W. These modes are responsible for the peaks at 812 and 818 cm^{-1} in the IR spectrum of the title compound [47].

The R6d block (Fig. 5) shows a short 230 cm^{-1} progression, formed by excitations of σ^+ metal–ligand stretch ν_5 in the Rydberg state, and two weak hot bands arising from excitations of this mode in the ground state. The ν_5 mode corresponds to the totally symmetric metal-ring stretching vibration in metallocenes and bis-arene complexes ($\nu = 311$ cm^{-1} in $(Cp)_2Fe$ [48] $\nu = 277$ cm^{-1} in $(Bz)_2Cr$ [49]). The intensity distribution in the R6d progression is usual for the Rydberg transitions originating at non-bonding MO (the strongest peak is due to the 0_0^0 excitation). The vibronic structure of the R6d block in the (Ch)(Cp)W spectrum is resolved even better than that of the lowest R*n*d band in the spectra of (Ch)(Cp)Cr and (Bz)(Cp)Mn [28–30], confirming the non-bonding character of the $5d(\sigma^+)$ MO in (Ch)(Cp)W and almost "pure" Rydberg nature of corresponding Rydberg state. The $5d(\sigma^+) \rightarrow R6d(\sigma^+)$ and $5d(\sigma^+) \rightarrow R6d(\pi)$ promotions are symmetry allowed in the $C_{\infty v}$ group. The R6d progression is similar to that observed for the $3d(\sigma^+) \rightarrow R4p(\pi)$ transition in (Ch)(Cp)Cr while the structure of the $R4s(\sigma^+)$ and $R4p(\sigma^+)$ excitations in the chromium complex are different. This fact as well as the large relative intensity of the R6d band (Fig. 1) make its assignment to the $5d(\sigma^+) \rightarrow R6d(\pi)$ transition preferable.

The R7p peak at 35930 cm^{-1} (Fig. 1) has the quantum defect (Table 2) appropriate for considering this feature as the second member of the $Rnp(\pi)$ series. Similar to the R6s and R6p bands, the (Ch)(Cp)W $R7p(\pi)$ transition is broadened in comparison with its (Ch)(Cp)Cr counterpart [28] owing to interaction with valence-shell excitations. However, the corresponding Rydberg state lies too high to mix with the excited levels derived from d–d transitions. So the $R7p(\pi)$ peak shows no spin–orbit splitting in contrast with the $R6p(\pi)$ band. The broadening of the $R7p(\pi)$ transition might be caused by an interaction with charge-transfer and ligand–ligand excitations responsible for bands A and B in the solution spectrum (Fig. 2).

Knowledge of the quantum defects of low-lying Rydberg transitions (Table 2) makes it possible to give more

detail assignment of higher Rydberg excitations in (Ch)(Cp)W. It is seen from Tables 2 and 3 that, for the $5d(\sigma^+) \rightarrow Rnp(\pi)$ promotions, δ decreases on going from the two lowest transitions to the higher members of series 1. Such a decrease in quantum defect is a typical phenomenon for sandwich molecules [23–30], being due to less penetration of high-lying Rydberg MOs into the molecular core [32,38] Similar effect should be expected for other Rydberg series in (Ch)(Cp)W. Comparison of Tables 2 and 3 shows that the interpretation of series 2 ($\delta = 3.04$) and series 3 ($\delta = 2.82$) as the $Rnp(\sigma^+)$ and $Rnd(\pi)$ transitions respectively is the most reasonable. Then the two remaining shoulders at 40430 and 40950 cm^{-1} can be assigned to the $R8d(\sigma^+)$ ($\delta = 2.89$) and $R9s(\sigma^+)$ ($\delta = 3.54$) excitations respectively. Thus the analysis of the (Ch)(Cp)W gas-phase photoabsorption has resulted in a complete interpretation of the Rydberg structure.

Acknowledgements

We thank the Royal Society for supporting this work. The research described in this publication was made possible in part by Grant N R8F000 from the International Science Foundation.

References

[1] J.C. Green, *Struct. Bonding (Berlin)*, 43 (1981) 37, and references cited therein.
[2] D.E. Cabelli, A.H. Cowley and J.J. Lagowskii, *Inorg. Chim. Acta*, 57 (1982) 195.
[3] F.G.N. Cloke, A.N. Dix, J.C. Green, R.N. Perutz and E.A. Seddon, *Organometallics, 2* (1983) 1150.
[4] C.E. Davies, I.M. Gardiner, J.C. Green, M.L.H. Green, N.J. Hazel, P.D. Grebenik, V.S. Mtetwa and K. Prout, *J. Chem. Soc., Dalton Trans.*, (1985) 669.
[5] T. Vondrak, *J. Organomet. Chem., 306* (1986) 89.
[6] G. Cooper, J.C. Green and M.P. Payne, *Mol. Phys., 63* (1988) 1031.
[7] J.A. Bandy, F.G.N. Cloke, G. Cooper, J.P. Day, R.B. Girling, R.G. Graham, J.C. Green, R. Grinter and R.N. Perutz, *J. Am. Chem. Soc., 110* (1988) 5039.
[8] D. O'Hare, J.C. Green, T.P. Chadwick and J.S. Miller, *Organometallics, 7* (1988) 1335.
[9] D.L. Lichtenberger and A.S. Copenhaver, *J. Chem. Phys., 91* (1989) 663.
[10] Yu. V. Chizhov, M.M. Timoshenko, L.P. Yur'eva, N.N. Zaitseva, I.A. Uralets, D.N. Kravtsov and N.L. Asfandiarov, *J. Organomet. Chem., 361* (1989) 79.
[11] T. Matsumura-Inoue, K. Kuroda, Y. Umezawa and Y. Achiba, *J. Chem. Soc., Faraday Trans. II*, 85 (1989) 857.
[12] J.G. Brennan, G. Cooper, J.C. Green, N. Kaltsonyannis, M.A. MacDonald, M.P. Payne, C.M. Redfern and K.H. Sze, *Chem. Phys., 164* (1992) 271.
[13] J.C. Green, M.L.H. Green, N. Kaltsonyannis, P. Mountford, P. Scott and S.J. Simpson, *Organometallics, 11* (1992) 3353.
[14] J.C. Green,N. Kaltsonyannis, K.H. Sze and M. MacDonald, *J. Am. Chem. Soc., 116* (1994) 1994.
[15] K.R. Gordon and K.D. Warren, *Inorg. Chem., 17* (1978) 987, and references cited therein.
[16] K.D. Warren, *Struct. Bonding (Berlin), 27* (1976) 45, and references cited therein.
[17] D.M. Duggan and D.N. Hendrickson, *Inorg. Chem., 14* (1975) 955.
[18] P. Grebenik, R. Grinter and R.N. Perutz, *Chem. Soc. Rev., 17* (1988) 453, and references cited therein.
[19] S.E.J. Bell, J.N. Hill, A. McCamley and R.N. Perutz, *J. Phys. Chem., 94* (1990) 3876.
[20] A. McCamley and R.N. Perutz, *J. Phys. Chem., 95* (1991) 2738.
[21] S. Yu. Ketkov and G.A. Domrachev, *Inorg. Chim. Acta, 178* (1990) 233.
[22] S. Yu. Ketkov and G.A. Domrachev, *J. Organomet. Chem., 420* (1991) 67.
[23] G.A. Domrachev, S. Yu. Ketkov and G.A. Razuvaev, *J. Organomet. Chem., 328* (1987) 341.
[24] S. Yu. Ketkov, G.A. Domrachev and G.A. Razuvaev, *Opt. Spectrosk., 63* (1987) 284.
[25] S. Yu. Ketkov, G.A. Domrachev, G.A. Razuvaev, L.P. Yur'eva and I.A. Uralets, *Organomet. Chem. USSR, 1* (1988) 500.
[26] S. Yu. Ketkov, G.A. Domrachev and G.A. Razuvaev, *J. Mol. Struct., 195* (1989) 175.
[27] S.Yu. Ketkov and G.A. Domrachev, *J. Organomet. Chem., 389* (1990) 187.
[28] S. Yu. Ketkov, *J. Organomet. Chem., 429* (1992) C38.
[29] S. Yu. Ketkov, *Opt. Spectrosk., 72* (1992) 595.
[30] S. Yu. Ketkov, *J. Organomet. Chem., 465* (1994) 225.
[31] M.L.H. Green, D.K.P. Ng and H.-V. Wong, *J. Chem. Soc., Dalton Trans.*, (1993) 3213.
[32] G. Cooper, J.C. Green, M.P. Payne, B.R. Dobson and I.H. Hillier, *J. Am. Chem. Soc., 109* (1987) 3836.
[33] F.S. Ham, *Phys. Rev. A, 138* (1965) 1727.
[34] M.D. Sturge, *Solid State Phys., 20* (1967) 92.
[35] L. Karlsson, R. Jadrny, L. Mattson, F.T. Chau and K. Siegbahn, *Phys. Scr., 16* (1977) 225.
[36] H. Lefebvre-Brion and R.W. Field, *Spectra of Diatomic Molecules*, Academic Press, New York, 1986.
[37] A. Bähr, G. Cooper, J.C. Green, K.A. Longley, M. Lovell-Smith and G.S. McGrady, submitted to *Chem. Phys.*
[38] J.C. Green, M.F. Guest, I.H. Hillier, S.A. Jarrett-Sprague, N. Kaltsoyannis, M.A. MacDonald and K.H. Sze, *Inorg. Chem., 31* (1992) 1588.
[39] B.E. Bursten, J.C. Green and N. Kaltsoyannis, *Inorg. Chem., 33* (1994) 2315.
[40] M.B. Robin, *Higher Excited States of Polyatomic Molecules*, Vol. 1, Academic Press, New York, 1974, 374 pp.
[41] R.S. Mulliken, *Phys. Rev., 57* (1940) 500.
[42] G. Herzberg, *Molecular Spectra and Molecular Structure*, Vol. III, *Electronic Spectra and Electronic Structure of Polyatomic Molecules*, Van Nostrand, New York, 1966.
[43] W.S. Felps, P. Hochmann, P. Brint and S.P. McGlynn, *J. Mol. Spectrosc., 59* (1976) 355.
[44] S.P. McGlynn, J.D. Scott, W.S. Felps and G.L. Findley, *J. Chem. Phys., 72* (1980) 421.
[45] W.S. Felps, J.D. Scott, G.L. Findley and S.P. McGlynn, *J. Chem. Phys., 74* (1981) 4832.
[46] M.B. Robin, *Higher Excited States of Polyatomic Molecules*, Vol. 3, Academic Press, Orlando, FL, 1985.
[47] H.W. Wehner, E.O. Fischer and J. Muller, *Chem. Ber., 103* (1970) 2258.
[48] D. Hartley and M.J. Ware, *J. Chem. Soc. A*, (1969) 138.
[49] S.J. Cyvin, J. Brunvoll and L. Schafer, *J. Chem. Phys., 54* (1971) 1517.